Ultrathin Shell Double Emulsion Templated Giant Unilamellar Lipid Vesicles with Controlled Microdomain Formation

*Laura R. Arriaga, Sujit S. Datta, Shin-Hyun Kim, Esther Amstad, Thomas E. Kodger, Francisco Monroy, and David A. Weitz**

***A** microfluidic approach is reported for the high-throughput, continuous production of giant unilamellar vesicles (GUVs) using water-in-oil-in-water double emulsion drops as templates. Importantly, these emulsion drops have ultrathin shells; this minimizes the amount of residual solvent that remains trapped within the GUV membrane, overcoming a major limitation of typical microfluidic approaches for GUV fabrication. This approach enables the formation of microdomains, characterized by different lipid compositions and structures within the GUV membranes. This work therefore demonstrates a straightforward and versatile approach to GUV fabrication with precise control over the GUV size, lipid composition and the formation of microdomains within the GUV membrane.*

1. Introduction

Giant unilamellar vesicles (GUVs), which are aqueous droplets stabilized by lipid bilayers, are useful model systems for the study of the physical properties of cell membranes;[1] however, this application depends critically on the ability of GUV bilayers to faithfully mimic cell membranes. For example, much like a cell membrane, the ultrathin bilayer of a GUV enables the robust encapsulation of biologically-relevant molecules or ions within its core. Moreover, when it is composed of a mixture of different lipids, a GUV membrane can exhibit spatial heterogeneities[2] that bear a striking resemblance to those observed in cell membranes.[3] An important example of this phenomenon is the phase separation of the lipids into well-defined microdomains characterized by different compositions and structures,[4] reminiscent of rafts in cell membranes;[5] these microdomains provide a powerful means to both assemble and regulate the function of key proteins,[6] and to tune the mechanical properties of the membrane as a whole.[5b] However, the physical characteristics or even the formation of microdomains in GUVs are highly sensitive to a bewildering array of factors, such as the lipid composition of the membrane, the presence of any residual solvents in the membrane, or the GUV size; these factors must thus be carefully controlled during GUV fabrication. Unfortunately, GUVs produced using conventional approaches, such as electroformation[7] and reverse emulsification,[8] vary widely in both their size and their composition, even within the same batch.[9] Microfluidic approaches can be used to produce GUVs with uniform sizes[10] and controlled lipid compositions;[10e,i,k] however, microdomain formation has not been observed in these GUVs. This is likely due to the presence of undesirable solvents, used during the fabrication process, that remain residually trapped within the GUV membranes.[11] These issues severely limit the use of GUVs for fundamental studies of microdomain formation.[9]

Dr. L. R. Arriaga, S. S. Datta, Prof. S.-H. Kim, Dr. E. Amstad, T. E. Kodger, Prof. D. A. Weitz
School of Engineering and Applied Sciences and Department of Physics
Harvard University
Cambridge, MA, 02138, USA
E-mail: weitz@seas.harvard.edu
Prof. S.-H. Kim
Department of Chemical and Biomolecular Engineering
KAIST, Daejeon, 305-701, South Korea
Prof. F. Monroy
Department of Physical Chemistry I
Complutense University
Madrid, 28040, Spain

DOI: 10.1002/smll.201301904

small NANO MICRO

It is therefore essential to develop an approach to GUV fabrication that enables control over the GUV size, lipid composition, and the formation of microdomains within the GUV membrane.

In this paper, we report a microfluidic approach for the continuous production of monodisperse GUVs using water-in-oil-in-water (W/O/W) double emulsion drops as templates. The middle oil phase is a mixture of the lipids that ultimately form the GUV membranes, dissolved in a mixture of a highly-volatile good solvent and a less volatile poor solvent. The shell formed by the middle phase around the aqueous double emulsion core is less than a micron thick,[12] much smaller than in typical double emulsion templates;[10e,k] this enables the fabrication of GUVs that contain minimal residual solvent within their membranes. The evaporation of the good solvent forces the bad solvent to dewet from the double emulsion drops, forming GUVs that stably encapsulate the material within their cores. By carefully controlling the lipid composition of the middle phase, we show that microdomains characterized by different compositions and structures[4] can form during the dewetting process; these microdomains are dynamic and fuse, ultimately resulting in the coexistence of two separate lipid phases. Our work thus demonstrates a straightforward approach to GUV fabrication that enables control over the GUV size, lipid composition, and the formation of microdomains within the GUV membrane.

2. Results and Discussion

2.1. Formation of W/O/W Double Emulsion Templates with Ultrathin Shells

We use a glass capillary microfluidic device to fabricate double emulsion drops with ultrathin shells.[12] The device consists of two tapered cylindrical capillaries, of outer diameter 1.00 mm, inserted into the opposite ends of a square capillary of inner diameter 1.05 mm; this configuration aligns the axes of the cylindrical capillaries. We then insert another smaller cylindrical capillary, of outer diameter approximately 200 μm, into the left tapered capillary, as illustrated in **Figure 1**. We use this smaller capillary to inject the innermost aqueous phase, an aqueous solution of 8 wt% poly(ethylene glycol) (PEG) and 2 wt% poly(vinyl alcohol) (PVA), into the left tapered capillary; the PEG enhances the viscosity of the solution, while the PVA enhances the stability of the double emulsion drops. Moreover, this polymer mixture enhances the optical contrast of the double emulsion cores in bright field microscopy. We treat the left tapered capillary with n-octadecyl-trimethoxy silane to render its surface hydrophobic, thus preventing wetting of the innermost aqueous phase on the capillary wall. We use this tapered capillary to inject the middle oil phase, a ternary lipid mixture of 35 mol% 1,2-dioleyl-sn-glycero-3-phosphocholine (DOPC), 35 mol% 1,2-dipalmitoyl-sn-glycero-3-phosphocholine (DPPC) and 30 mol% cholesterol, dissolved in a mixture of 36 vol% chloroform and 64 vol% hexane; the total lipid concentration is 5 mg/mL. We inject both the innermost aqueous phase and the middle oil phase at a flow rate of 500 μL/h; under these conditions the innermost aqueous phase forms large water-in-oil emulsion drops within the left tapered capillary, as exemplified in the schematic illustration in Figure 1. We then inject the outer aqueous phase, a 10 wt% PVA solution, through the interstices between the left tapered capillary and the square capillary, at a flow rate of 5000 μL/h. We treat the right tapered capillary with 2-[methoxy (polyethyleneoxy) propyl] trimethoxy silane to render its surface hydrophilic, thus preventing wetting of the middle oil phase on its wall. This protocol forces the water drops to become re-emulsified, forming monodisperse W/O/W double emulsion drops with ultrathin shells at the orifice of the right tapered capillary, as shown in Figure 1 and Movie S1 of the Supporting Information. Our ability to produce such an ultrathin oil phase is not specific to a particular choice of fluid phases, provided that the inner and outer fluid viscosities are in the right ratio; nor is it specific to a particular flow rate, provided that the device is operated in the discontinuous dripping regime. Instead, it directly reflects the design of our glass-capillary device. In particular, it relies on the chemical functionalization of the capillary surfaces.[12] To prevent osmotic stresses, we collect the drops thus produced in a sucrose solution having the same osmolarity as the inner water cores.

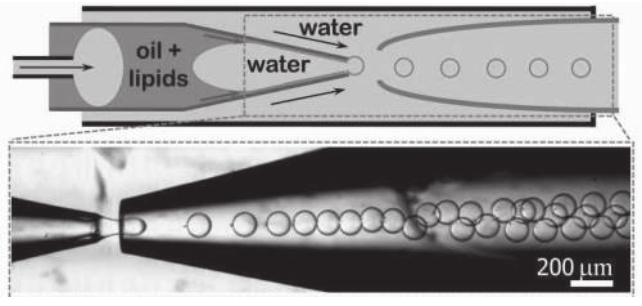

Figure 1. Microfluidic fabrication of water-in-oil-in-water double emulsion drops with ultrathin shells.

2.2. Dewetting-Induced Formation of the Lipid Bilayer

We use these double emulsion drops as templates for GUV formation. Unfortunately, templates with thick shells do not form GUVs; instead, they form capsules with heterogeneous shells comprised of aggregated material.[13] Importantly, our templates have ultrathin shells; this feature enables GUV formation. All of our experiments are performed at room temperature. Unlike hexane, the chloroform in the ultrathin double emulsion shell is a good solvent for the lipids, enabling them to remain fully dissolved during double emulsion formation. The lipids also adsorb to the interfaces between the inner core, ultrathin shell, and the outer aqueous phase, thereby reducing the interfacial energy, as illustrated in **Figure 2**(a). Crucially, however, the chloroform is more soluble in water and evaporates more rapidly than the hexane,[14] turning the shell into a hexane-rich poor solvent for the lipids. The reduction in the solvent quality induces an attractive interaction between the two lipid monolayers at the interfaces of the ultrathin shell,[15] forcing them to stick

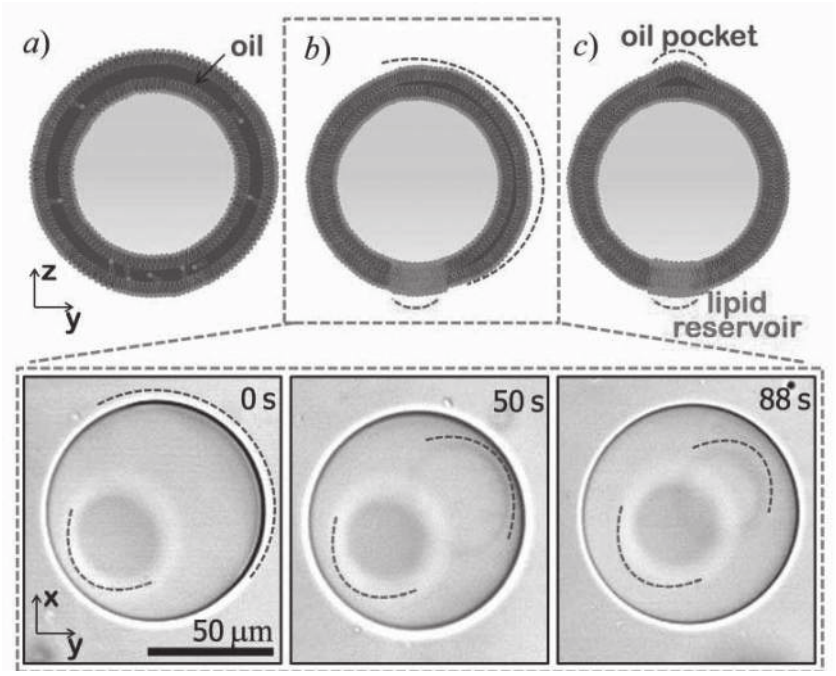

Figure 2. Illustration (not to scale) of (a) a double emulsion template, (b) the formation of the lipid bilayer through dewetting of the middle oil phase, also shown in the optical micrographs and (c) the resultant GUV, which contains a minuscule oil pocket at the top and eventually a lipid reservoir at the bottom.

together and form a bilayer membrane when a random fluctuation bring them closer; this ultimately triggers a dewetting transition, similar to that observed in the microfluidic production of polymersomes,[16] that occurs over a duration of just a couple of minutes, as shown in Figure 2(b). Because the remaining solvent is less dense than the inner aqueous core, it forms a minuscule oil pocket at the top of the double emulsion, as illustrated in Figure 2(b-c), and as shown in the optical micrographs in Figure 2. This oil pocket then evaporates, producing a stable GUV.

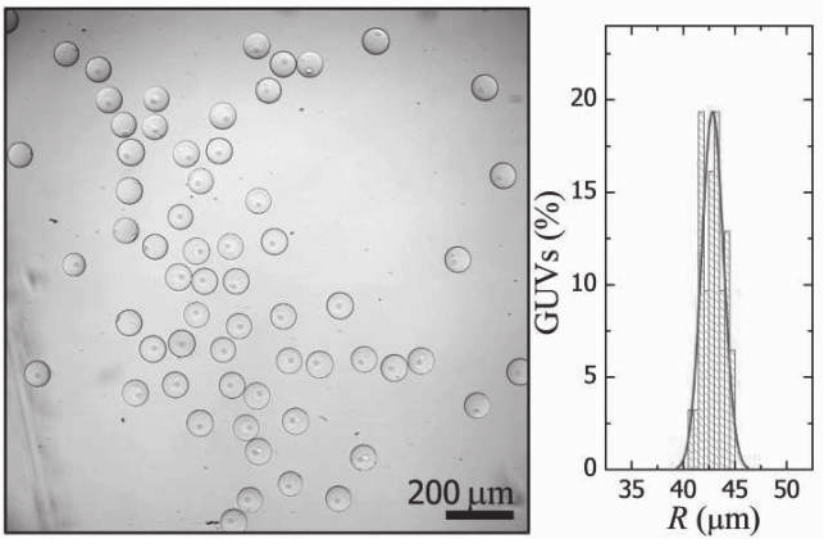

Figure 3. Optical microscope image of the resultant GUVs and their radius distribution.

We frequently observe the formation of a small lipid reservoir at the bottom of each GUV, as shown in Figure 2, and also visible in **Figure 3**; this provides the GUV with the ability to swell without inducing additional stresses in its membrane, as shown in Movie S2 of the Supporting Information. Owing to the precise control over the size of the double emulsion drops used as templates, the resultant GUVs are highly monodisperse, with radius 42 ± 1 μm, as shown in Figure 3.

2.3. Unilamellarity of the Vesicle Membrane

We expect the GUVs thus formed to be impermeable to small molecules. To test this, we add sulforhodamine, at a final concentration of 14 μg/mL, to the outer sucrose phase. We incubate the GUVs for 50 min to ensure the homogeneous distribution of the sulforhodamine molecules by diffusion, and then monitor the evolution of the fluorescence intensity within the GUV core and in the outer phase, I_{core} and I_{outer}, respectively. Consistent with our expectation, we do not observe a significant change in the fluorescence intensity or radius of the GUV, as exemplified in **Figure 4**(a) and shown by the solid symbols in Figure 4(c); this confirms that its membrane is impermeable to sulforhodamine.

To further characterize the structure of the GUV membrane, we incorporate a pore-forming membrane protein, α-hemolysin (α-HL), into it; the transmembrane segment of this protein spans a single bilayer in size, as schematized in the illustration of Figure 4(b). Thus, α-HL only forms pores in unilamellar membranes. We add α-HL to the outer phase at a final concentration of 7 μg/mL, and incubate the vesicle for 20 min; under these conditions, α-HL spontaneously incorporates itself into the GUV membrane, driven by the hydrophobic interactions between its hydrophobic region and the inner, hydrophobic region of the lipid bilayer.[10c,g],[17] Subsequently, we expose the GUV to a sucrose solution of 14 μg/mL sulforhodamine. In stark contrast to the previous case, I_{core}/I_{outer} increases over time at a markedly faster rate, as exemplified in Figure 4(b) and shown by the open symbols in Figure 4(c); this reflects the penetration of sulforhodamine into the vesicle core, confirming that our vesicles are unilamellar. Interestingly, the GUV concomitantly swells, as shown in Figure 4(b); this reflects the flow of water into the GUV core. We hypothesize

NANO MICRO small

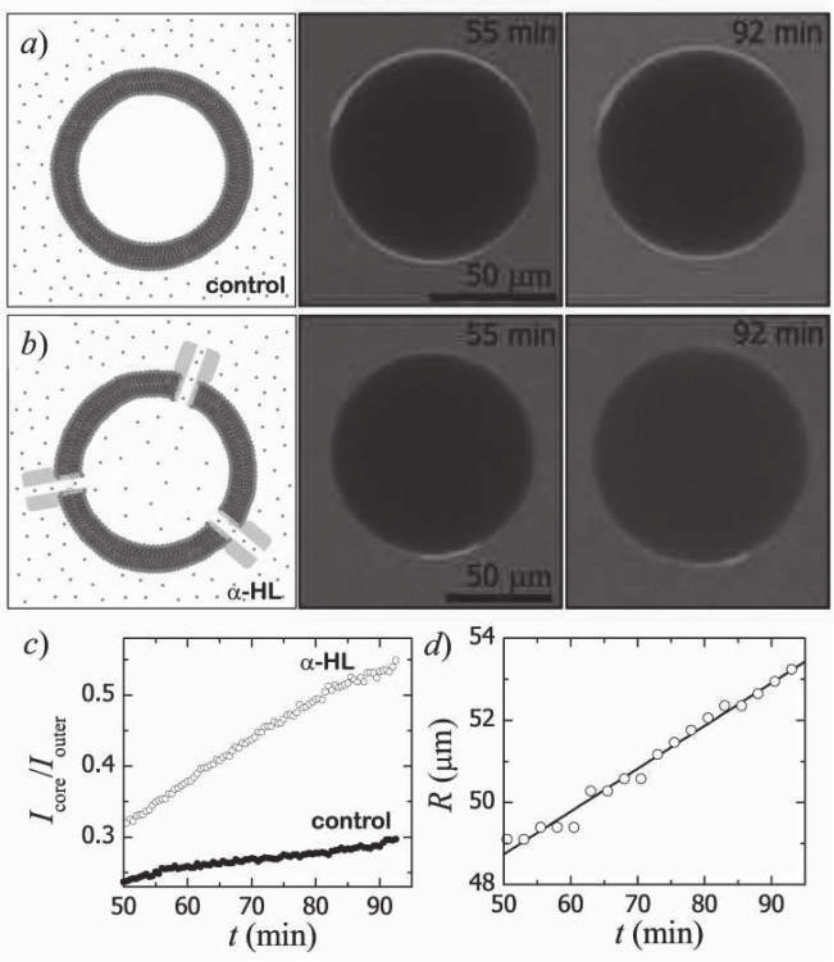

Figure 4. (a-b) Illustration (not to scale) and confocal microscope images of GUVs exposed to sulforhodamine in the (a) absence and (b) presence of the pore-forming protein α-HL. (c) Variation with time of the intensity of the GUV core relative to the outer phase, in the presence and absence of α-HL. Both GUVs exhibit a small amount of fluorescence in their core even in the absence of sulforhodamine, due to the fluorescent dyes used to label the GUV membrane; this results in a non-zero initial value of I_{core} for the control. (d) Variation with time of the radius of the GUV containing α-HL; no variation is measured for the control. Time t in (c-d) indicates time elapsed after addition of sulforhodamine.

that this inflow is driven by the penetration of the sulforhodamine and sucrose into the GUV core, which initially contains a high concentration of large PVA and PEG molecules at an osmolarity matched to that of the outer phase.[18] These polymers are too large to diffuse through the GUV membrane, even when it contains α-HL pores, and remain in the GUV core; by contrast, the small sucrose and sulforhodamine molecules in the outer phase do diffuse through the α-HL pores, to equilibrate their chemical potentials.[19] In doing so, they transiently raise the osmotic pressure inside the GUV core; this drives the co-flow of water into the core, as well.[20] Within this picture the GUV radius should increase in time as $R(t) \approx R_0 + P_S t$,[21] where R_0 is the initial GUV radius and P_S quantifies the permeability of the α-HL-containing GUV membrane to small molecules, as detailed in the Supporting Information. We use our optical micrographs to quantify this behavior. Consistent with the theoretical expectation, the GUV radius increases linearly, as shown in Figure 4(d); fitting these data to the theoretical expression yields a measurement of the permeability, $P_S = 1.5 \pm 0.1$ nm/s. Interestingly, we do not observe that the GUV swelling stops over the experimental time period; instead, we observe that GUVs which are left to swell for much longer time periods eventually rupture.

2.4. Formation of Membrane Microdomains

When composed of a suitable mixture of different lipids, a GUV membrane should exhibit microdomain formation;[4] however, this phenomenon has not been observed in GUVs produced using microfluidics. To form microdomains in the GUV membranes, we carefully control the lipid composition of the double emulsion middle phase. The ternary lipid mixture that we use is known to phase separate into two different types of microdomains characterized by different molecular structures and compositions: liquid disordered (ld) domains, which are enriched in DOPC, and liquid ordered (lo) domains, which are enriched in DPPC and cholesterol.[4] We distinguish the different domains by incorporating two different fluorescent dyes into the lipid mixture, 0.25 mol.% DHPE-rhodamine and 0.75 mol.% naphtopyrene; these selectively associate with the ld and lo domains, respectively.[4c] As the chloroform evaporates from the double emulsion shell, the lipids adsorbed to the interfaces between the inner core, ultrathin shell, and the outer phase form microdomains at each of these interfaces; this is shown in the first frame of **Figure 5**(a). These microdomains are highly dynamic and often fuse, as shown in the subsequent three frames of Figure 5(a). The ultrathin shell of the double emulsion then dewets from the innermost aqueous cores, as shown in the last two frames of Figure 5(a), forming a GUV that initially contains multiple ld and lo microdomains over its entire surface; the complete process is shown in Movie S3 of the Supporting Information. Three optical sections, taken at three different depths within such a GUV, are shown in Figure 5(b). Interestingly, these domains continue to fuse, thereby minimizing the line energy between their boundaries,[2c] eventually forming two distinct ld and lo microdomains, as exemplified by the three optical sections shown in Figure 5(c). These microdomains are circular in shape, similar to those observed in GUVs prepared using conventional methods. Moreover, they are highly monodisperse, as shown in **Figure 6**, in stark contrast to the large variability in microdomain sizes observed in GUVs prepared using conventional methods, exemplified by Figure S1 of the Supporting Information. This reflects the exquisite

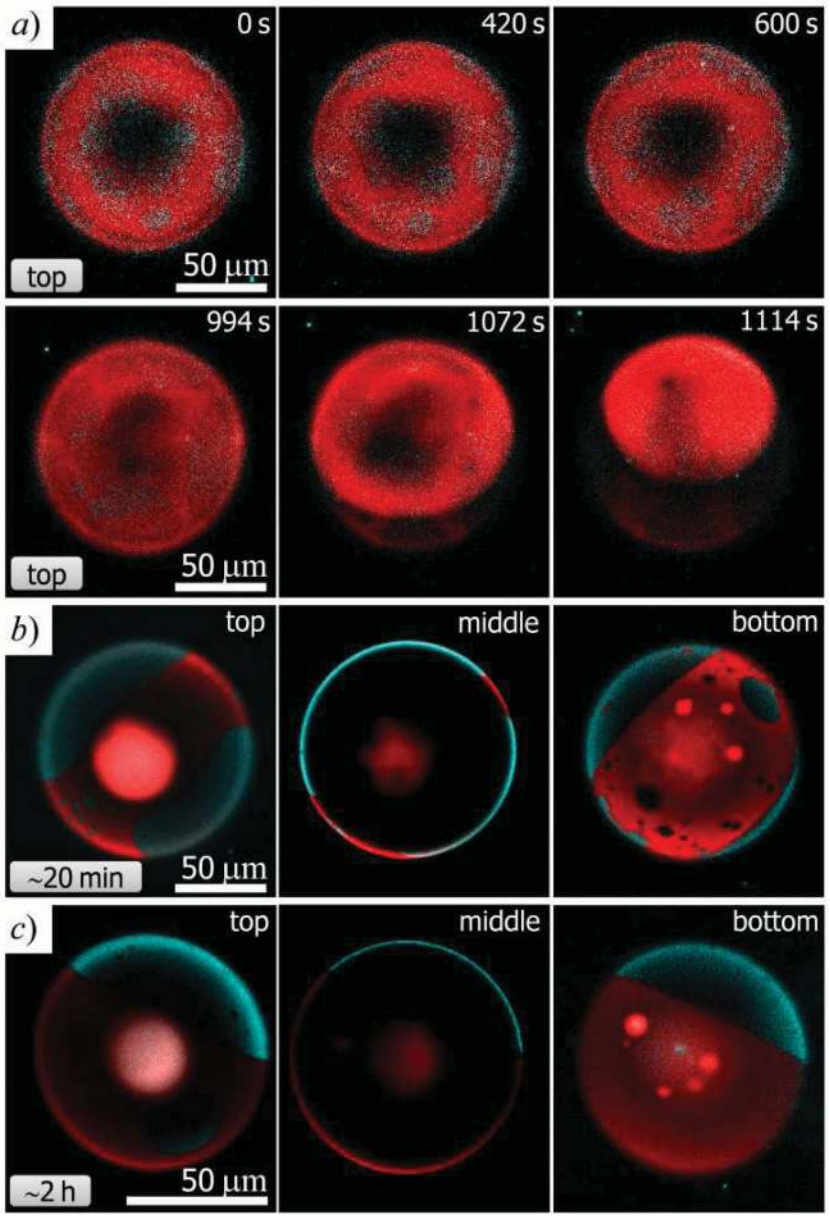

Figure 5. Overlayed confocal images of the DHPE-Rh (red) and naphtopyrene (blue) channels, which selectively associate with the liquid disordered and liquid ordered microdomains, respectively. (a) Time sequence of optical sections corresponding to the top plane of a double emulsion drop during its transformation into a GUV. (b) Different optical sections, taken at different depths, of the GUV immediately after the dewetting process. (c) Different optical sections of the GUV after fusion of the microdomains, yielding a minimum-energy structure.

control over the lipid compositions and GUV sizes afforded by our approach. These observations thus highlight the utility of forming GUVs from ultrathin shell double emulsion templates.

3. Conclusion

Our microfluidic approach provides a versatile way to produce GUVs having carefully controlled sizes and lipid compositions. We produce these GUVs using double emulsion drops as templates; the drops have ultrathin shells, resulting in GUVs that contain a minimal amount of residual solvent within their membranes. This enables us to produce GUVs whose membranes can, for appropriate mixtures of lipids, phase separate into microdomains; these microdomains are dynamic and often fuse, resulting in minimum-energy structures. The microdomains can have differing permeabilities;[22] thus, controlling the fraction of the different microdomains may be a promising means of tuning the overall GUV permeability. Unlike other fabrication approaches, ours is high throughput, enabling the continuous production of large quantities of GUVs whose membranes exhibit microdomain formation. Moreover, our approach can be used to produce GUVs using a broad range of lipid compositions; this is in stark contrast to approaches that rely on the fusion of different vesicles, each composed of a single lipid.[9] Such a fusion process precludes the incorporation of many biologically-relevant lipids, such as cholesterol, which cannot form vesicles, into the GUV membranes. Our work thus describes a route to produce GUVs that provide a useful model system for the study of the physical properties of cell membranes.

4. Experimental Section

Materials: We conduct our experiments with the following lipids: 1,2-dioleoyl-sn-glycero-3-phosphocholine (DOPC), 1,2- dipalmitoyl-sn-glycero-3-phosphocholine (DPPC) (Avanti Polar Lipids, Inc.) and cholesterol (Sigma-Aldrich Co.). As fluorescent probes, we use 1,2-dioleoyl-sn-glycero-3-phosphoethanolamine-N-(lissamine rhodamine B sulfonyl) (DHPE-Rh) (Molecular Probes) and naphtopyrene (Sigma). We use mixtures of chloroform and hexane (Sigma) as solvent for the lipids. For the aqueous phases, we dissolve poly(ethylene glycol) (PEG, Mw = 6 kDa, Sigma) and poly(vinyl alcohol) (PVA, Mw = 13–23 kDa, Sigma) in milli-Q water (Millipore, resistivity of 18.2 MΩ/cm) to 10 wt.%; these solutions are filtered through 5 μm filters (Acrodisc) and mixed to the desired volume fractions before their injection in the microfluidic device. We also prepare 100 mM aqueous solutions of sucrose (VWR) to collect the emulsion droplets. Details of the experiments performed to optimize GUV fabrication are explained in the Supporting Information.

We conduct our unilamellarity tests using α-Hemolysin (α-HL) from Staphylococcus aureus (Sigma). We dissolve the lyophilized powder of α-HL, which contains sodium cytrate buffer, in milli-Q water to a concentration of 0.5 mg/mL; this solution is diluted to

NANO MICRO small

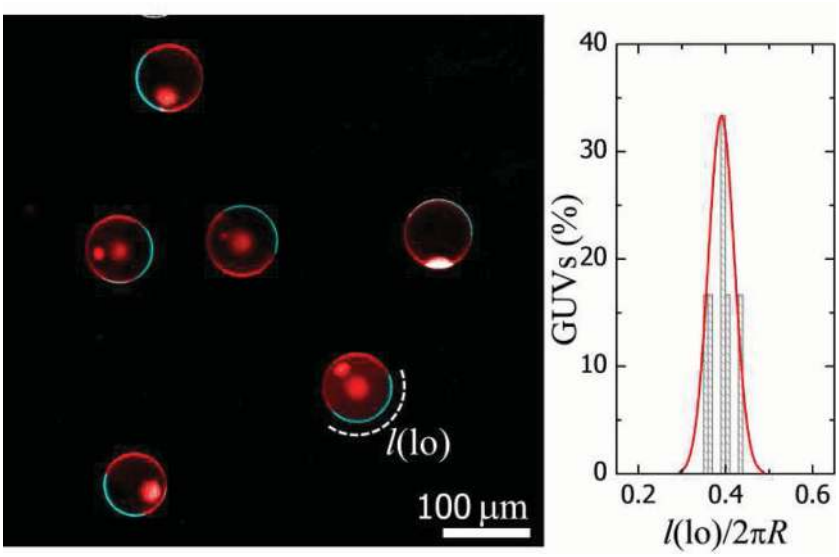

Figure 6. Overlayed confocal fluorescent image of GUVs with liquid disordered and liquid ordered microdomains and distribution of the fraction of the GUV perimeter taken up by the liquid ordered domain.

0.025 mg/mL for the experiments. To test the permeability of the GUV membranes to small molecules, we dissolve sulforhodamine B (Sigma) in a 100 mM sucrose solution to a final concentration of 0.1 mg/mL. Both the α-HL and sulforhodamine solutions are diluted further upon addition to the suspension containing the GUVs to final concentrations of 7 and 14 μg/mL, respectively.

Osmolarity: We carefully adjust the osmolarity of the inner, outer and collection phases to 100 mOsm/L; this avoids any osmotic stress in the process of GUV formation from double emulsion drops. The measurements are performed using a Micro-Osmometer (Advanced Instruments, Inc.)

Fabrication of the Glass Capillary Device:[12] The device consists of two cylindrical capillaries (World Precision Instruments, Inc.), of inner and outer diameters 0.58 mm and 1.00 mm, respectively, inserted into the opposite ends of a square capillary (Atlantic International Technology, Inc.) of inner dimension 1.05 mm; this configuration aligns the axes of the cylindrical capillaries. We taper these cylindrical capillaries to a diameter of 20 μm with a micropipette puller (P-97, Sutter Instrument, Inc.) and then carefully sand them to final diameters of 80 and 120 μm. We treat the capillary with smaller diameter with n-octadecyl-trimethoxy silane (Aldrich) to render its surface hydrophobic and the capillary with larger diameter with 2-[methoxy (polyethyleneoxy) propyl] trimethoxy silane (Gelest, Inc.) to render its surface hydrophilic. We stretch a third cylindrical capillary with a burner to an outer diameter of approximately 200 μm. We assemble the device onto a glass microscope slide. For this, we fix the square capillary to the slide with 5 minute® Epoxy (Devcon). Then, we insert the two tapered capillaries in the opposite ends of the square capillary, the one with smaller diameter on the left and the one with larger diameter on the right. We align them on the microscope maintaining a separation distance between them of approximately 100 μm and fix them to the slide with epoxy. Next, we insert the small stretched capillary into the left cylindrical capillary. Finally, we place dispensing needles (Type 304, McMaster Carr) at the junctions between capillaries or their ends, and fix them to the slide with epoxy. We use these needles to inject the different liquid phases that ultimately form the emulsion drops.

Operation of the Microfluidic Device: We pour the inner and outer aqueous phases into 10 mL plastic syringes (Becton) and the middle oil phase into a 5 mL glass syringe (Hamilton). We connect the dispensing needles of the syringes to the dispensing needles of the device with polyethylene tubing of inner diameter 0.86 mm (Scientific Commodities, Inc.). We inject the liquid phases at constant flow rates using pumps (Harvard Apparatus). We work in the discontinuous dripping regime;[12] this regime produces single emulsion drops and double-emulsion drops with ultrathin shells intermittently. The single emulsion drops are separated from the double emulsion drops with ultrathin shells upon collection, due to their different density. We collect the drops in a 10–20 × volumetric excess of sucrose solution; therefore, single emulsion drops float in the collection vial and are removed with a Pasteur pipette, whereas double-emulsion drops with ultrathin shells rapidly sink because they are heavier than the sucrose solution.

Imaging: We record the production of double emulsion drops within the microfluidic device using a 5× objective on an inverted microscope (Leica) equipped with a high speed camera (Phantom V9). We monitor the formation of the GUVs from the double emulsion drops using bright field and confocal fluorescence microscopy. Using a 10× dry objective with a numerical aperture of 0.3 on a confocal microscope (Leica), we acquire bright field and two-channel fluorescence images, simultaneously, using multi-track mode. For this, we use Argon (458 nm) and HeNe (543 nm) lasers as excitation sources for the naphtopyrene and the DHPE-Rh, respectively; the fluorescence emission is collected by the PMT detectors through bandpass filters between 460 and 530 nm for the naphtopyrene channel, and between 560 and 670 nm for the DHPE-Rh channel. In addition, the contrast provided by the presence of PEG and PVA in the inner cores of the GUVs allows us to visualize them in bright field. All our experiments are performed at room temperature. For the images, we place the double emulsion templates or the resultant GUVs in between two micro cover glasses (VWR) separated and sealed using high vacuum grease (Dow Corning) at the edges for imaging.

Supporting Information

Supporting Information is available from the Wiley Online Library or from the author.

Acknowledgements

This work was supported by Amore-Pacific, the NSF (DMR-1006546) and the Harvard MRSEC (DMR-0820484). L. R. A. was

supported by Real Colegio Complutense. S. S. D. acknowledges support from ConocoPhillips and E. A. from the Swiss National Foundation (PBEZP2-137304).

[1] a) R. Lipowsky, E. Sackman, *Structure and Dynamic of Membranes: From Cells to Vesicles*, Elsevier, **1995**; b) S. P. Desai, M. D. Vahey, J. Voldman, *Langmuir* **2009**, *25*, 3867.
[2] a) C. Dietrich, L. A. Bagatolli, Z. N. Volovyk, N. L. Thompson, M. Levi, K. Jacobson, E. Gratton, *Biophys. J.* **2001**, *80*, 1417; b) S. L. Veatch, S. L. Keller, *Phys. Rev. Lett.* **2002**, *89*, 268101; c) T. Baumgart, S. T. Hess, W. W. Webb, *Nature* **2003**, *425*, 821; d) T. Hamada, Y. Miura, Y. Komatsu, Y. Kishimoto, M. D. Vestergaard, M. Takagi, *J. Phys. Chem. B* **2008**, *112*, 14678; e) E. Greco, G. Quintiliani, et al. *Proc. Natl. Acad. Sci. USA* **2012**, *109*, E1360.
[3] Y. Yoon, P. J. Lee, S. Kurilova, W. Cho, *Nat. Chem.* **2011**, *3*, 868.
[4] a) S. L. Veatch, I. V. Polozov, K. Gawrish, S. L. Keller, *Biophys. J.* **2007**, *93*, 539; b) R. F. M. de Almeida, J. Borst, A. Fedorov, M. Prieto, A. J. W. G. Visser, *Biophys. J.* **2007**, *93*, 539; c) P. Husen, L. R. Arriaga, F. Monroy, J. H. Ipsen, L. A. Bagatolli, *Biophys. J.* **2012**, *103*, 2304.
[5] a) K. Simons, E. Ikonen, *Nature* **1997**, *387*, 569; b) D. Lingwood, K. Simons, *Science* **2010**, *327*, 46.
[6] M. A. Lemmon, *Nat. Rev. Mol. Cell. Biol.* **2008**, *9*, 99.
[7] a) M. I. Angelova, D. S. Dimitrov, *Faraday Discuss.* **1986**, *81*, 303; b) M. I. Angelova, S. Soleau, P. Meleard, F. Faucon, P. Bothorel, *Prog. Coll. Pol. Sci.* **1992**, *89*, 127.
[8] a) S. Pautot, B. J. Frisken, D. A. Weitz, *Langmuir* **2003**, *19*, 2870; b) S. Pautot, B. J. Frisken, D. A. Weitz, *Proc. Natl. Acad. Sci. USA* **2003**, *100*, 10718.
[9] R. Dimova, S. Aranda, N. Bexlyepkina, V. Nikolov, K. A. Riske, R. Lipowsky, *J. Phys.: Condens. Matter* **2006**, *18*, S1151.
[10] a) Y.-C. Tan, K. Hettiarachchi, M. Siu, Y.-R. Pan, A. P. Lee, *J. Am. Chem. Soc.* **2006**, *128*, 5656; b) K. Funakoshi, H. Suxuki, S. Takeuchi, *J. Am. Chem. Soc.* **2007**, *129*, 12608; c) J. C. Stachowiak, D. L. Richmond, T. H. Li, A. P. Liu, S. H. Parekh, D. A. Fletcher, *Proc. Natl. Acad. Sci. USA* **2008**, *105*, 4697; d) S. Sugiura, T. Kuroiwa, T. Kagota, M. Nakajima, S. Sato, S. Mukataka, P. Walde, S. Ichikawa, *Langmuir* **2008**, *24*, 4581; e) H. C. Shum, D. Lee, I. Yoon, T. Kodger, D. A. Weitz, *Langmuir* **2008**, *24*, 7651; f) J. C. Stachowiak, D. L. Richmond, T. H. Li, F. Brochard-Wyart, D. A. Fletcher, *Lab Chip* **2009**, *9*, 2003; g) S. Ota, S. Yoshizawa, S. Takeuchi, *Angew. Chem. Int. Ed.* **2009**, *48*, 6533; h) S. Matosevic, B. M. Paegel, *J. Am. Chem. Soc.* **2011**, *133*, 2798; i) D. L. Richmond, E. M. Schmid, S. Martens, J. C. Stachowiak, N. Liska, D. A. Fletcher, *Proc. Natl. Acad. Sci. USA* **2011**, *108*, 9431; j) P. C. Hu, S. Li, N. Malmstadt, *ACS Appl. Mater. Interfaces* **2011**, *3*, 1434; k) S.-Y. Teh, R. Khnouf, H. Fan, A. P. Lee, *Biomicrofluidics* **2011**, *5*, 044113; l) K. Nishimura, H. Suzuki, T. Toyota, T. Yomo, *J. Colloid. Interface Sci.* **2012**, *376*, 119.
[11] D. van Swaay, A. deMello, *Lab Chip* **2013**, *13*, 752.
[12] S.-H. Kim, J. W. Kim, J.-C. Cho, D. A. Weitz, *Lab Chip* **2011**, *11*, 3162.
[13] T. Foster, K. D. Dorfman, H. T. Davis, *J. Colloid. Interface Sci.* **2010**, *351*, 140.
[14] The chloroform likely saturates the inner core, and then proceeds to diffuse out of the double emulsion, into the outer aqueous phase. We expect that, as evaporation proceeds, the chloroform that saturates the core also continues to diffuse out.
[15] A. R. Thiam, N. Bremond, J. Bibette, *Langmuir* **2012**, *28*, 6291.
[16] a) R. C. Hayward, A. S. Utada, N. Dan, D. A. Weitz, *Langmuir* **2006**, *22*, 4457; b) H. C. Shum, J.-W. Kim, D. A. Weitz, *J. Am. Chem. Soc.* **2008**, *130*, 9543; c) H. C. Shum, E. Santanach-Carreras, J.-W. Kim, A. Ehrlicher, J. Bibette, D. A. Weitz, *J. Am. Chem. Soc.* **2011**, *133*, 4420.
[17] a) R. Hemmler, G. Bose, R. Wagner, R. Peters, *Biophys. J.* **2005**, *88*, 4000; b) L. C. M. Gross, O. K. Catell, M. I. Wallace, *Nano Lett.* **2011**, *11*, 3324.
[18] We expect that solely redistributing the excess lipids in the membrane would not lead to the isotropic swelling that we observe, which also requires the inflow of water. Instead, such a redistribution, without water inflow, would increase the GUV surface area without increasing its volume, likely leading to enhanced shape fluctuations of the GUV membrane, which we do not observe. Rather, in our experiments, the lipid redistribution is concomitant with GUV swelling.
[19] While it is possible that based on its size, the sucrose can *leave* the vesicles through the α-HL pores, we do not expect this to be the case: because the concentration of the sucrose, and hence its chemical potential, is larger in the outer phase, this drives it to primarily flow into the GUV core.
[20] M.-T. Lee, W.-C. Hung, F.-Y. Chen, H. W. Huang, *Proc. Natl. Acad. Sci. USA* **2008**, *105*, 5087.
[21] a) O. Kedem, A. Katchalsky, *Biochim. Biophys. Acta* **1958**, *27*, 229; b) P. Peterlin, V. Arrigler, H. Diamant, D. Haleva, *Adv. Planar Lipid Bilayers Liposomes* **2012**, *16*, 301.
[22] J. C. Mathai, S. Tristam-Nagle, J. F. Nagle, M. L. Zeidel, *J. Gen. Physiol.* **2008**, *131*, 69.

Received: June 20, 2013
Revised: August 14, 2013
Published online: October 22, 2013

